

MOL #88567

Role of JunB in Adenosine A_{2B} Receptor-mediated VEGF Production

Sergey Ryzhov, Asel Biktasova, Anna E. Goldstein, Qinkun Zhang, Italo Biaggioni,

Mikhail M. Dikov, Igor Feoktistov

Divisions of Cardiovascular Medicine (QZ, IF, SR) and Clinical Pharmacology (AEG,
IB),

Departments of Cancer Biology (AB, MMD), Medicine (AEG, QZ, IB, IF, SR) and
Pharmacology (IB, IF)

Vanderbilt University, Nashville, TN 37232.

MOL #88567

Running Title: *Adenosine and JunB in VEGF production*

Corresponding authors: Igor Feoktistov, MD, PhD, 360 PRB, Vanderbilt University, 2220 Pierce Ave, Nashville, TN 37232-6300. Phone: 615-936-1732, FAX: 615-936-1733, email: igor.feoktistov@vanderbilt.edu; Sergey Ryzhov, MD, PhD, 360 PRB, Vanderbilt University, 2220 Pierce Ave, Nashville, TN 37232-6300. Phone: 615-936-1733, FAX: 615-936-1733, email: sergey.v.ryzhov@vanderbilt.edu

Number of text pages: 42

Number of tables: 1

Number of figures: 9

Number of references: 54

Number of words in the Abstract: 245

Number of words in the Introduction: 468

Number of words in the Discussion: 1017

Abbreviations:

The abbreviations used are: BSA, bovine serum albumin; Ca/DAG-GEF, calcium diacylglycerol guanine nucleotide exchange factor; CRE, cyclic AMP-responsive element; ChIP, chromatin immunoprecipitation; DAG, diacylglycerol; DAPI, 4',6-diamidino-2-phenylindole; DMEM, Dulbecco's modified Eagle's medium; DNJunB, dominant negative mutant of JunB; ERK, extracellular signal-regulated kinase; IP₃, inositol trisphosphate; HIF-1, hypoxia-inducible factor-1; LLC, Lewis lung carcinoma; mCSC, mouse cardiac Sca-1⁺CD31⁻ stromal cells; MEK, mitogen-activated protein kinase kinase; NECA, 5'-N-ethylcarboxamidoadenosine; PBS, phosphate buffered saline; PKC, protein kinase C; PKA, protein kinase A; PMA, phorbol 12-myristate 13-acetate; PLC, phospholipase C; Rp-cAMPS, Rp-adenosine 2',5'-cyclic monophosphorothioate; Rap1, Ras-proximate-1; RT-PCR, reverse transcription-polymerase chain reaction; shRNA, short hairpin RNA; VEGF, vascular endothelial growth factor

MOL #88567

ABSTRACT

Interstitial adenosine stimulates neovascularization in part through A_{2B} adenosine receptor-dependent upregulation of vascular endothelial growth factor (VEGF). In the current study, we tested the hypothesis that A_{2B} receptors upregulate JunB, which can contribute to stimulation of VEGF production. Using human microvascular endothelial cell line HMEC-1, human mast cell line HMC-1, mouse cardiac Sca1-positive stromal cells, and mouse Lewis lung carcinoma (LLC) cells, we found that adenosine receptor-dependent upregulation of VEGF production was associated with an increase in VEGF transcription, AP-1 activity and JunB accumulation in all cells investigated. Furthermore, the expression of JunB, but not the expression of other genes encoding transcription factors from the Jun family, was specifically upregulated. In LLC cells expressing A_{2A} and A_{2B} receptor transcripts, only the nonselective adenosine agonist NECA, but not the selective A_{2A} receptor agonist CGS21680, significantly increased JunB reporter activity and JunB nuclear accumulation, which were inhibited by the A_{2B} receptor antagonist PSB603. Using activators and inhibitors of intracellular signaling, we demonstrated that A_{2B} receptor-dependent accumulation of JunB protein and VEGF secretion share common intracellular pathways. NECA enhanced JunB binding to the murine VEGF promoter, whereas mutation of the high-affinity AP-1 site (-1093 to -1086) resulted in a loss of NECA-dependent VEGF reporter activity. Finally, NECA-dependent VEGF secretion and reporter activity were inhibited by the expression of a dominant negative JunB or by JunB knockdown. Thus, our data suggest an important role of the A_{2B} receptor-dependent upregulation of JunB in VEGF production and possibly other AP-1-regulated events.

MOL #88567

INTRODUCTION

The endogenous nucleoside adenosine is an intermediate product of adenine nucleotide metabolism. It is accumulated at sites of tissue injury, inflammation and local hypoxia. This results in increased local adenosine concentrations in the interstitium, where it exerts its actions via binding to extracellular G protein-coupled adenosine receptors, namely A₁, A_{2A}, A_{2B} and A₃ (Fredholm et al., 2001). Adenosine has long been known to stimulate VEGF production and angiogenesis (for reviews see (Adair, 2005; Feoktistov et al., 2009)). In particular, we demonstrated that stimulation of A_{2B} adenosine receptors upregulated VEGF secretion in various cell types including cardiac mesenchymal stem-like cells (Ryzhov et al., 2012), retinal and skin endothelial cells (Grant et al., 1999; Grant et al., 2001; Feoktistov et al., 2002), certain types of cancer cells (Zeng et al., 2003; Ryzhov et al., 2008a), tumor-infiltrating hematopoietic cells (Ryzhov et al., 2008a), and mast cells (Feoktistov and Biaggioni, 1995; Feoktistov et al., 2003; Ryzhov et al., 2008b). Although adenosine signaling through hypoxia-inducible factor-1 (HIF-1), a key transcription factor responsible for the tissue adaptation to ischemia, has been studied in detail (Merighi et al., 2005; Merighi et al., 2006; De Ponti et al., 2007; Ramanathan et al., 2007; Alchera et al., 2008; Ramanathan et al., 2009; Gessi et al., 2010), the role of other transcription factors in the adenosine-dependent VEGF production is not known. In addition to HIF-1, several transcription factor-binding sites for AP-1, AP-2, Erg-1, Sp1/Sp3, and STAT-3 have been identified within a 1.2 kb region of both mouse and human VEGF promoters (for review see (Pages and Pouyssegur, 2005)). The AP-1 transcription factor family is composed of proteins belonging to the Jun (c-Jun, JunB, and Jun D) subfamily proteins that can bind to AP-1

MOL #88567

consensus sites either in their homodimeric forms or upon forming heterodimeric complexes with members of the Fos or the ATF subfamilies of AP-1 proteins (for review see (Karin et al., 1997)). There is growing evidence suggesting an important non-redundant role of JunB in the regulation of VEGF production and angiogenesis. When the different Jun members were deleted in mice, only the loss of JunB affected vascular development (Schorpp-Kistner et al., 1999). More recent studies have demonstrated that JunB can bind directly to an AP-1 consensus sequence within a 1.2 kb region of the mouse VEGF promoter and upregulate VEGF production in response to hypoxia or hypoglycemia independently of HIF-1 signaling (Textor et al., 2006; Schmidt et al., 2007). It is not known, however, if JunB is involved in the adenosine-dependent regulation of VEGF production. To the best of our knowledge, the effects of adenosine on members of Jun subfamily of AP-1 proteins, including JunB, have not been reported yet.

In the current study, we tested the hypothesis that A_{2B} adenosine receptors upregulate JunB, which can contribute to stimulation of VEGF production and possibly many other AP-1-dependent events.

MOL #88567

MATERIALS AND METHODS

Reagents. 8-[4-[4-((4-chlorophenyl)piperazine-1-sulfonyl)phenyl]]-1-propylxanthine (PSB603) was from Tocris Bioscience (Bristol, UK). 5'-N-ethylcarboxamidoadenosine (NECA) and 2-p-(2-carboxyethyl) phenylethylamino-NECA (CGS 21680) were purchased from Research Biochemicals, Inc. (Natick, MA). Phorbol 12-myristate 13-acetate (PMA), forskolin, Rp-adenosine 2',5'-cyclic monophosphorothioate (Rp-cAMPS) were from Sigma (St. Louis, MO). N-[2-((p-bromocinnamyl) amino)ethyl]-5-isoquinolinesulfonamide, dihydrochloride (H89), 1-(6-{{[17 β -3-methoxyestra-1,3,5-(10)triene-17-yl] amino}hexyl)-1H-pyrrole-2,5-dione (U73122), 1-(6-{{[17 β -3-methoxyestra-1,3,5-(10)triene-17-yl] amino}hexyl)-2,5-pyrrolidine-dione (U73343), 1,4-diamino-2,3-dicyano-1,4-bis(2-aminophenylthio)butadiene (UO126), 1,4-diamino-2,3-dicyano-1,4-bis(methylthio)butadiene (UO126), and 3-[1-[3-(Dimethylamino)propyl]-5-methoxy-1H-indol-3-yl]-4-(1H-indol-3-yl)-1H-pyrrole--2,5-dione (Gö6983) were purchased from Calbiochem (San Diego, CA). Cell culture media were purchased from Invitrogen Corporation (Carlsbad, CA). Mouse basic fibroblast growth factor was obtained from ProSpec-Tany Technogene, Ltd. (East Brunswick, NJ). Mouse interferon- γ was purchased from R&D Systems (Minneapolis, MN). Fetal bovine serum (FBS), non-essential amino acids, Antibiotic-Antimycotic solution, α -thioglycerol, and dimethyl sulfoxide were purchased from Sigma (St. Louis, MO). When used as a solvent, final dimethyl sulfoxide concentrations in all assays did not exceed 0.1% and the same dimethyl sulfoxide concentrations were used in vehicle controls.

Cell culture. Human microvascular endothelial cells (HMEC-1), obtained from Centers for Disease Control and Prevention/National Center for Infectious Diseases (Atlanta,

MOL #88567

GA), were grown in 199 medium containing 15% FBS and supplemented with 30 $\mu\text{g}/\text{mL}$ endothelial cell growth supplement (BD Biosciences, San Jose, CA). Human mast cell line (HMC-1) was a gift from Dr. Joseph H. Butterfield (Mayo Clinic, Rochester, MN). HMC-1 cells were maintained in suspension culture at a density between 3 and 6×10^5 cells/ml by dilution with Iscove's medium supplemented with 10% FBS, 2 mM glutamine and 1.2 mM α -thioglycerol. Lewis lung carcinoma (LLC) cells (CRL-1642) were obtained from American Type Culture Collection (Manassas, VA) and maintained in 10% FBS DMEM medium. HEK293T cells were purchased from Thermo Fisher Scientific (Waltham, MA) and maintained in DMEM-High Glucose supplemented with 10% FBS and 2 mM glutamine. Mouse cardiac Sca-1⁺CD31⁻ stromal cells (mCSC) were isolated as previously described (Ryzhov et al., 2012). Cells were propagated on 0.1% gelatin-coated tissue culture dishes in DMEM-High Glucose supplemented with 10% FBS, 2 mM glutamine, 10 ng/ml basic fibroblast growth factor and 10 ng/ml interferon- γ at 33°C. Three days before experiments, cells were replated and cultured in the absence of interferon- γ at 37°C.

Real-time Reverse Transcription-Polymerase Chain Reaction (RT-PCR). Total RNA was isolated from cells using RNeasy Mini kit (Qiagen, Valencia, CA). One microgram of total DNase-treated RNA was used to generate cDNA with MMLV RT (Promega, Madison, WI) and random hexamers (Applied Biosystems, Foster City, CA). RT-PCR was carried using ABI PRISM 7900HT Sequence Detection System (Applied Biosystems, Foster City, CA) as described previously (Ryzhov et al., 2012). Primer pairs for human and murine adenosine receptors (A_1 , A_{2A} , A_{2B} , A_3) were obtained from Applied Biosystems (human AdoRs: Hs00181231, Hs00169123, Hs00386497,

MOL #88567

Hs00181232 and murine AdoRs: Mm01308023, Mm00802075, Mm00839292 and Mm00802076). Primer sequences for human and mouse JunB, JunD, c-Jun and β -actin are listed in Table 1.

Western Blot analysis. Cells were lysed in RIPA buffer containing protease inhibitors cocktail (Roche Diagnostics, Indianapolis, IN). Total protein concentrations were quantified with Pierce BCA Protein Assay Kit (Pierce Biotechnology, Rockford, IL). Equal amounts of protein (30-60 μ g/well) were resolved in NuPAGE® Novex® 4-12% Bis-Tris polyacrylamide gel in the presence 1X MES buffer (Invitrogen) and transferred to a polyvinylidene fluoride membrane Immobilon-FL (Millipore Bioscience Research Reagents, Temecula, CA). Rabbit polyclonal anti-JunB (sc-73), anti-ERK (sc-154), goat polyclonal phospho-ERK antibody (sc-7976) and mouse monoclonal anti- β -actin (sc-69879) were used at 1:750, 1:500, 1:200 and 1:1000 dilutions, respectively (all from Santa Cruz Biotechnology, Santa Cruz, CA). Anti- β -Tubulin (DM1B) antibody (Millipore) was used at a concentration of 0.2 μ g/ml (1:5000 dilution). After treatment with an appropriate peroxidase-conjugated secondary antibody, the bands were visualized with an enhanced chemiluminescence method (Nesbitt and Horton, 1992). The intensity of protein bands was quantified by a densitometer using ImageJ 1.45s software (National Institutes of Health, Bethesda, MD). In some experiments, secondary anti-mouse IRDye@800CW (1:8000) and anti-rabbit IRDye@680LT (1:20000) antibodies (Li-Cor Bioscience, Lincoln, NE) were used. The blots were scanned with LICOR Odyssey Infrared imager (Li-Cor Bioscience, Lincoln, NE) to visualize fluorescent immunocomplexes.

MOL #88567

Immunofluorescence microscopy. LLC cells were seeded into glass 8-chamber slides and grown to 90-95% confluency. Cells were incubated in the presence of reagents indicated under *Results* for 6 h and fixed in 4% paraformaldehyde containing 0.1% Triton X-100. Cells were permeabilized with 0.3% Triton X-100 and blocked with 3% BSA in PBS. Cells were incubated with rabbit anti-JunB (sc-73, Santa Cruz Biotechnology) antibody overnight at 4°C, washed and incubated with AlexaFluor488-conjugated donkey anti-rabbit IgG (Molecular Probes, Eugene OR) at 1:1000 dilution for 2 h. The slides were mounted with ProLong® Gold Antifade reagent with DAPI (Invitrogen). Images were acquired with Olympus FV-1000 inverted confocal microscope using a 100X/1.40 SPlan-UApo oil immersion objective and excitation/emission wavelengths of 405 and 488, and processed using F10-ASW 1.6 Viewer. Corrected total cell fluorescence (CTCF) values were calculated as Integrated Density – (Area of selected cell x Mean fluorescence of background readings) using ImageJ 1.45s software (National Institutes of Health).

Chromatin immunoprecipitation (ChIP) assay. The ChIP Assay was performed using SimpleChIP® Enzymatic Kit (Cell Signaling Technology, Danvers, MA) according to the manufacturer's instructions. Briefly, LLC cells (2×10^7 per immunoprecipitation) were cross-linked using formaldehyde. Cell nuclei were isolated after sonication (7 times with 20 sec pulses on ice) using Sonic Dismembrator 300 (Thermo Fisher). Equal amounts of chromatin were immunoprecipitated with JunB antibody (sc-73, Santa Cruz Biotechnology, Inc.). Rabbit IgG was used as negative control. After reversal of crosslinks and DNA purification, PCR amplification was performed using Mastercycler® gradient thermal cycler (Eppendorf, Hamburg, Germany). Forward primer 5'-

MOL #88567

AGCTGGCCTACCTACCTTTCTGA-3' and reverse primer 5'-CTTATCTGAGCCCTTGTCTG-3' were used for amplification of the VEGF gene promoter region from -1140 to -733 harboring the putative AP-1 site (Schmidt et al., 2007), employing the following conditions: 94°C for 4 min; 30–35 cycles at 94°C for 30 sec, 58.5°C for 30 sec, and 72°C for 30 sec; and final extension at 72°C for 10 min. The PCR products were analyzed on a 1.5% agarose gel.

Constructs and Luciferase Reporter assays. To construct mouse JunB promoter-driven luciferase reporter (pJunB-luc), mouse genomic DNA was isolated using DNeasy Blood & Tissue kit (Qiagen). The JunB genomic DNA, comprising 5' flanking -870 to +133 base pairs of the murine JunB gene, was generated using PCR. MluI and XhoI restriction sites were introduced into forward: 5'- GAGGTACAGCCTCACGCGTACAA -3' and reverse primers: 5'- AGTTGGCTCGAGTGC GTAAAGGC -3'. After digestion with MluI and XhoI, the 1.0-kb PCR fragment was ligated upstream of a promoterless luciferase gene into the *KpnI-XhoI* sites of pGL2-basic vector (Promega). The sequence was verified against published database-accessible sequences. pAP1-luc reporter was purchased from Agilent Technologies, Inc. (Santa Clara, CA). Mouse VEGF promoter-driven luciferase reporter, which encompasses 1.2 kb of the 5'-flanking sequence, the transcription start site, and 0.4-kb of corresponding 5'-UTR (Shima et al., 1996) was kindly provided by Dr. Patricia A. D'Amore (Harvard University, Boston MA). Mouse VEGF luciferase reporter with the putative AP-1 site at position -1093 to -1086 mutated from TGAATCA to AGGTTCC (Schmidt et al., 2007) was kindly provided by Dr. Marina Schorpp-Kistner (DKFZ - German Cancer Research Center, Heidelberg, Germany). Human VEGF promoter-driven luciferase reporter VEGF-P7 (Forsythe et al.,

MOL #88567

1996) was kindly provided by Dr. Greg L. Semenza (Johns Hopkins Hospital, Baltimore, MD). Dominant negative JunB mutant construct pcDNA3-JunB Δ N (Ikebe et al., 2007), was a kind gift from Dr. Mitsuyasu Kato (University of Tsukuba, Japan). Cells were grown to 50% confluency and transfected with 1 μ g/well of plasmid DNA using Fugene[®]HD reagent (Roche). To test the effect of dominant negative JunB mutant on VEGF reporter activity, pcDNA3-JunB Δ N, pVEGF-luc and pRL-SV40 vectors were cotransfected at ratio 80:20:1. Twenty-four hours after transfections, cells were incubated in the presence of reagents indicated under *Results* for an additional 6 h. Reporter activity was measured using a Dual-Luciferase Reporter Assay System (Promega). Firefly luciferase reporter activities were normalized against *Renilla* luciferase activities from the coexpressed pRL-SV40 and expressed as relative luciferase activities over the basal level.

Stable transfection of dominant negative JunB mutant in LLC cells. LLC cells were transfected with pcDNA3-JunB Δ N or empty pcDNA3 plasmid. After 24h, growth medium was replaced with a fresh medium containing 0.8 mg/ml G-418. One week later, colonies of LLCs survived after G-418 treatment were selected and the expression of dominant negative JunB mutant was verified by Western immunoblotting using rabbit polyclonal anti-JunB (sc-73, Santa Cruz Biotechnology).

Production and stable transduction of lentiviral vectors encoding short hairpin RNA (shRNA) in LLC cells. MISSION[®] pLKO.1-puro JunB shRNA1 (TRCN0000232241), shRNA2 (TRCN0000232242), shRNA3 (TRCN0000054488), shRNA4 (TRCN0000042698), shRNA5 (TRCN0000042699), empty vector (SHC001), and non-targeting control non-mammalian shRNA (SHC002) plasmids were purchased from Sigma-Aldrich. Lentiviral psPAX.2 packaging (Cat. #12260) and pMD2.G (Cat. #12259)

MOL #88567

envelope plasmids were obtained from Addgene (Cambridge MA). HEK293T were co-transfected with MISSION[®] pLKO.1-puro, psPAX.2 and pMD2.G plasmid constructs using Lipofectamine 2000 (Invitrogen). Virus-containing supernatants were harvested 48h later and frozen at -80°C . For infection, LLC cells (2×10^5 per well) were seeded on 6-well plates and 12 h later were incubated with lentiviral particles diluted 1:1000 in DMEM medium containing 10% FBS and 8 $\mu\text{g}/\text{mL}$ Polybrene (Sigma) for an additional 12h. After 36h recovery, stably transduced LLC cells were selected by culturing in the presence of 2 $\mu\text{g}/\text{ml}$ puromycin (Sigma).

Evaluation of Ras-proximate-1 (Rap1) activation. After overnight serum starvation, HMEC-1 cells were incubated in the absence or presence of 10 μM U73122 for 30 min followed by incubation in the presence of 10 μM NECA for 5, 10 or 15 min. Rap1 activation was determined after pull-down of Rap1-GTP with GST-RalGDS-Rap1 binding domain using Active Rap1 Pull-Down and Detection Kit (Thermo Fisher Scientific) following the supplier's instructions.

Analysis of VEGF secretion. VEGF protein level in culture media was measured using an enzyme-linked immunosorbent assay kit (R&D Systems).

Statistical analysis. Data were analyzed using GraphPad Prism 4.0 software (GraphPad Software, San Diego, CA) and presented as mean \pm SEM. Comparisons between several treatment groups were performed using one-way ANOVA, followed by appropriate post hoc tests. Comparisons between two groups were performed using two-tailed unpaired *t* tests. A *p* value < 0.05 was considered significant.

MOL #88567

RESULTS

JunB accumulation and increase in AP-1 activity are associated with adenosine-dependent upregulation of VEGF production in different human and mouse cell types.

To determine the potential involvement of JunB in adenosine-dependent stimulation of VEGF production we chose two human cell lines, HMEC-1 and HMC-1, and two mouse cell lines, mCSC and LLC, in all of which the A_{2B} receptor dependent-regulation of VEGF secretion has been described (Feoktistov et al., 2002; Feoktistov et al., 2003; Ryzhov et al., 2012; Ryzhov et al., 2008a). Figure 1 demonstrates that stimulation of adenosine receptors with 10 μM NECA for 6 hours significantly increased VEGF release (panels A-D) from all cells studied. To determine whether the upregulation of VEGF production by NECA occurs at the transcriptional level, two mouse cell lines mCSC and LLC were transiently transfected with a mouse VEGF promoter-driven luciferase reporter, which encompasses 1.2 kb of the 5'-flanking sequence that includes AP-1 binding sites previously proven to physically interact with JunB (Schmidt et al., 2007). Human cell lines HMEC-1 and HMC-1 were transiently transfected with a homologous human VEGF promoter-driven luciferase reporter. Figure 1 (panels E-H) shows that stimulation of adenosine receptors with 10 μM NECA for 6 hours significantly increased luciferase expression in all cells investigated, indicating that upregulation of VEGF production by NECA can occur at the transcriptional level. Next, we tested if stimulation with NECA increases AP-1 reporter activity. We transiently transfected cells with the AP-1 luciferase reporter construct pAP-1-luc that contains seven times repeated AP-1-binding sites. Figure 1 (panels J-M) shows that stimulation of adenosine receptors with

MOL #88567

10 μ M NECA for 6 hours significantly increased luciferase expression in all cells investigated.

In parallel to stimulation of AP-1 and VEGF reporters, Western blot analysis of JunB protein content in cell lysates showed that stimulation of adenosine receptors with 10 μ M NECA for 3 hours significantly increased JunB protein accumulation in all cells investigated (Figure 1, panels N-Q). Furthermore, we found that NECA significantly upregulated the expression of JunB but not the expression of other genes encoding transcription factors from the Jun family (Figure 2).

A_{2B} adenosine receptors promote JunB expression at the transcriptional level and increase accumulation of JunB protein in the nucleus.

The expression of A_{2B} receptors is a common feature of all cells investigated in this study. Figure 3A compares the results of real-time RT-PCR analysis of the expression of mRNA encoding subtypes of adenosine receptors in HMEC-1, HMC-1, mCSC and LLC cell lines. In addition to the expression of A_{2B}, all cells also expressed A_{2A} receptor transcripts with A_{2A}/A_{2B} receptor ratio lowest in LLC and highest in HMC-1 cells. No other receptor subtype transcripts were detected in these cells except for HMC-1 expressing A₃ receptors in addition to A_{2A} and A_{2B} receptors.

To determine whether stimulation of A_{2B} adenosine receptors can promote JunB expression at the transcriptional level, LLC cells were transiently transfected with a mouse JunB promoter-driven luciferase reporter, which encompasses 5' flanking -870 to +133 base pairs. Figure 3B shows that only the nonselective adenosine agonist NECA (10 μ M) but not the selective A_{2A} receptor agonist CGS 21680 (1 μ M) significantly increased the reporter activity, and this effect was inhibited by the A_{2B} receptor

MOL #88567

antagonist PSB603 (Borrmann et al., 2009) at a selective concentration of 100 nM. PSB603 inhibited JunB protein levels in a concentration-dependent manner in whole lysates of LLC cells stimulated with 10 μ M NECA for 3 hours (Figure 3C). Furthermore, stimulation of A_{2B} adenosine receptors promoted JunB accumulation specifically in the cell nucleus. As seen in Figure 3D, only faint immunofluorescence staining with anti-JunB antibody was detected in the nuclei of control cells (Basal), contrasting with the strong fluorescence present in the nuclei of NECA-treated cells after 3 hours of treatment. No JunB staining was detected in the cytoplasm. The NECA-induced nuclear accumulation of JunB was reduced to nearly basal levels in the presence of 100 nM PSB603. Quantitative analysis of the immunofluorescence data confirmed a significant increase in JunB staining in cells stimulated with NECA in the absence but not in the presence of PSB603 (Figure 3E). Taken together, our data suggest that stimulation of A_{2B} receptors can activate the nuclear factor JunB at the transcriptional level, with subsequent accumulation of this protein in the nucleus.

A_{2B} receptor-dependent upregulation of JunB expression and VEGF secretion share common intracellular pathways.

We chose HMEC-1 cells to conduct pharmacological analysis of intracellular pathways involved in the adenosine-dependent regulation of JunB protein expression and VEGF secretion because of their robust responses to stimulation of adenosine receptors (Figure 1A, N). These cells express A_{2A} and A_{2B} but not A₁ or A₃ adenosine receptor transcripts (Figure 3A). The nonselective adenosine agonist NECA (10 μ M) induced VEGF secretion (Figure 4A) and increased JunB protein accumulation (Figure 4B, C). In contrast, the A_{2A} receptor agonist CGS 21680 had no effect when used at a selective

MOL #88567

concentration of 1 μM (Figure 4A-C). A_{2B} receptors in HMEC-1 cells are known to couple to Gs and Gq proteins resulting in accumulation of cAMP and diacylglycerol (DAG)/inositol trisphosphate (IP_3) (Feoktistov et al., 2002). As seen in Figure 4, stimulation of cAMP-dependent pathways with 1 μM forskolin or DAG-dependent pathways with 10 nM PMA increased both JunB protein expression and VEGF secretion.

To explore the role of cAMP/protein kinase A (PKA) signaling pathways in adenosine-dependent upregulation of JunB and VEGF, HMEC-1 cells were stimulated with 10 μM NECA in the presence of PKA inhibitors. In ancillary experiments, we monitored cAMP/PKA signal transduction by the activity of luciferase reporter under control of tandem repeats of the cAMP-responsive elements (CRE) transiently expressed in HMEC-1 cells. We estimated that the PKA inhibitor H-89 inhibited the activity of NECA-stimulated CRE reporter with an IC_{50} value of 3.2×10^{-7} M (Supplemental figure 1). However, 1 μM H-89 had little if any effect on VEGF release induced by 10 μM NECA (Figure 5A). Furthermore, another PKA inhibitor Rp-cAMPS with a different mechanism of action and reported IC_{50} values in a low micromolar range (Rothermel et al., 1983) had also no effect on NECA-induced VEGF secretion at concentrations up to 10^{-4} M (Figure 5A). These results suggest that adenosine actions on VEGF release are PKA-independent. To explore a potential role of protein kinase C (PKC) signaling pathways in adenosine-dependent upregulation of JunB and VEGF, we tested effects of the broad-spectrum inhibitor of PKC Gö6983, with reported IC_{50} values for most isoforms in a low nanomolar range (Gschwendt et al., 1996), on NECA-induced VEGF secretion. We found that 1 μM Gö6983 had no effect on NECA-induced VEGF secretion (Figure 5A). These results suggest that Gö6983-sensitive PKC isoforms play no role in

MOL #88567

NECA-induced VEGF secretion. In parallel to their lack of effects on NECA-induced VEGF release, the PKA inhibitors H-89 (1 μ M) and Rp-cAMPS (100 μ M), and the PKC inhibitor Gö6983 (1 μ M) had also no effect on NECA-induced JunB protein accumulation in HMEC-1 cells (Figure 5B-C).

We next evaluated a potential role of alternative signaling pathways in A_{2B} receptor-dependent VEGF production by using inhibitors of phospholipase C (PLC)- β (Figure 6A) and mitogen-activated protein kinase kinase (MEK)1/2 (Figure 6B). From these experiments we chose concentrations of inhibitors to test their effects on A_{2B} receptor-dependent JunB protein accumulation (Figure 6C, D). To explore the role of A_{2B} receptor-Gq-linked PLC- β pathways in adenosine-dependent upregulation of VEGF, we used the PLC inhibitor U73122 and its succinimido analogue U73343 as a negative control (Bleasdale et al., 1990). Figure 6A shows that U73122 at concentrations of 1-10 μ M produced a greater inhibition of NECA-stimulated VEGF release from HMEC-1 compared to U73343. Similar difference between U73122 and U73343 in their inhibitory actions on JunB protein accumulation was observed when these compounds were added at concentrations of 10 μ M before stimulation of HMEC-1 cells with NECA (Figure 6C, D).

We have previously reported that inhibition of MEK1/2 with UO126 partially reduced A_{2B} receptor-dependent VEGF production in human and mouse mast cells (Ryzhov et al., 2008b). Therefore, we compared the effects of MEK1/2 inhibition on NECA-induced VEGF release and JunB protein accumulation in HMEC-1 cells. As seen in Figure 6B, the MEK1/2 inhibitor UO126 at concentrations of 1-10 μ M inhibited VEGF release by approximately 50%. In contrast, the inactive form of MEK1/2 inhibitor UO124

MOL #88567

had no effect on NECA-dependent VEGF secretion at concentrations up to 10 μ M. Similarly, 1 μ M UO126 produced partial inhibition of NECA-induced JunB protein accumulation, whereas 1 μ M UO124 had no effect (Figure 6C, D). However, UO126 at this concentration almost completely blocked extracellular-signal-regulated kinase (ERK) activity (Supplemental figure 2). Taken together, our data suggest that ERK1/2 activated by MEK1/2 may be partially responsible not only for NECA-induced VEGF release but also for JunB protein accumulation.

Calcium diacylglycerol guanine nucleotide exchange factor (CalDAG-GEF) – Rap1 pathway has been implicated in PMA-dependent ERK activation, thus providing a potential link between PLC and ERK (Stork and Dillon, 2005). To determine whether stimulation of adenosine receptors leads to PLC-dependent activation of Rap1 in HMEC-1, we stimulated cells with 10 μ M NECA in the absence or presence of 10 μ M U73122 and measured Rap1 activation. As seen in Figure 7, stimulation of adenosine receptors with NECA indeed induces transient activation of Rap1. The NECA-induced activation of Rap1 was considerably lower in the presence of the PLC inhibitor U73122.

JunB binding to the VEGF promoter is an important step in the A_{2B} receptor-dependent stimulation of VEGF production.

Previous studies have identified the AP-1 recognition site located at position -1093 to -1086 of the murine VEGF promoter as the only high-affinity JunB-binding site and demonstrated that JunB acts primarily through this element to stimulate VEGF transcription during hypoxia (Schmidt et al., 2007). To prove that stimulation of A_{2B} receptors induces physical interaction of JunB with the VEGF promoter, CHIP analysis was performed in LLC cells incubated in the absence or presence of 10 μ M NECA.

MOL #88567

Primers were designed to amplify the region of the VEGF promoter (-1140 to -733) containing the high-affinity AP-1 site. We found weak basal JunB binding to this promoter region in the absence of NECA, which was considerably enhanced in cells stimulated with NECA (Figure 8A). To demonstrate the requirement of JunB binding to the high-affinity AP-1 site for the A_{2B} receptor-dependent stimulation of VEGF transcription, we used a luciferase reporter analysis. As seen in Figure 8B, mutation of the high-affinity AP-1 site (-1093 to -1086) within the murine promoter fragment resulted in a loss of stimulation of luciferase activity by NECA. To further ascertain the role of JunB in the A_{2B} receptor-dependent regulation of VEGF transcription, a plasmid encoding dominant negative mutant of JunB (DNJunB) or an empty expression vector (mock transfection) was co-transfected with VEGF promoter-driven luciferase reporter in LLC cells. Twenty-four hours after transfection, cells were incubated in the presence or absence of 10 μ M NECA for an additional 6 hours. Figure 8B shows that the expression of DNJunB significantly suppressed NECA-stimulated reporter activity.

To further demonstrate the role of JunB in A_{2B} receptor-dependent regulation of VEGF secretion, we established LLC colonies that either stably expressed DNJunB or underwent mock transfection with an empty vector. DNJunB protein expression was confirmed by Western blotting (Figure 8C). Images of full-length gels are shown in Supplemental figure 3. We found that the stable expression of DNJunB resulted in significant suppression of NECA-induced VEGF secretion (Figure 8C). It should be noted that the expression of DNJunB also affected basal VEGF secretion to some extent. However, a relative increase in VEGF secretion induced by NECA was still considerably

MOL #88567

lower in cells expressing DNJunB compared with mock-transfected control (1.5- and 2-fold, respectively).

Finally, we used an RNA interference approach to evaluate the effect of JunB knockdown on the A_{2B} receptor-dependent VEGF production. Based on Western blot analysis of efficacy of JunB silencing after stable lentiviral transfection of LLC cells with different JunB shRNA constructs (shRNA1-5, Figure 8E), we selected cells expressing shRNA5 for further experiments. We confirmed that both basal and NECA-induced JunB mRNA levels were largely suppressed in LLC cells expressing shRNA5 compared with cells expressing non-targeting control shRNA (Figure 8F). We found that JunB knockdown resulted in significant suppression of NECA-induced VEGF secretion (Figure 8G) similar to that seen in cells expressing DNJunB (Figure 8D). Taken together, our results suggest that JunB plays an important role in the A_{2B} receptor-dependent regulation of VEGF transcription.

MOL #88567

DISCUSSION

Our study demonstrated for the first time that JunB protein accumulation is induced in response to stimulation of A_{2B} adenosine receptors in different types of murine and human cells. A_{2B} receptor-dependent regulation of JunB abundance can occur at the transcriptional level as evidenced from stimulation of a JunB reporter by the adenosine analog NECA, which was blocked by the selective A_{2B} receptor antagonist PSB603. Stimulation with NECA induced a robust increase in JunB transcripts in all cells under investigation. In contrast, the expression of c-Jun was rather downregulated by NECA albeit to a different extent depending on the cell type. NECA had little if any effect on the expression of JunD. Thus, our results suggest that of all members of the Jun subfamily, JunB is the principal target of A_{2B} receptor signaling. Using an AP-1 reporter, we confirmed that adenosine-dependent increase in JunB results in formation of functional AP-1 proteins in these cells.

AP-1 proteins have been implicated in the induction of VEGF expression by ultraviolet B irradiation in fibroblasts (Dong et al., 2012), by hyperbaric oxygen in endothelial cells (Lee et al., 2006), and by tumor necrosis factor α in breast cancer cells (Yin et al., 2009). Because physical interaction of JunB with AP-1 binding sites of the VEGF promoter and subsequent stimulation of VEGF secretion have been previously demonstrated in fibroblasts and endothelial cells upon stimulation with hypoxia (Schmidt et al., 2007) or hypoglycemia (Textor et al., 2006), our new findings raised a possibility that JunB can be involved also in the upregulation of VEGF by A_{2B} receptor signaling. We investigated signaling pathways linked to A_{2B} receptors that may lead to JunB protein accumulation and VEGF secretion in HMEC-1 cells (Figure 9). These cells express

MOL #88567

mRNA encoding A_{2A} and A_{2B} receptors, but not other adenosine receptor subtypes. Both A_{2A} and A_{2B} receptors are known to be coupled to Gs proteins linked to stimulation of adenylate cyclase and accumulation of cAMP (Fredholm et al., 2001). However, we have previously shown that only A_{2B} receptors are functionally coupled to adenylate cyclase in these cells because only NECA but not the selective A_{2A} agonist CGS 21680 stimulated cAMP accumulation (Feoktistov et al., 2002). In agreement with these data, CGS 21680 had no effect on either JunB or VEGF.

In various cells including HMEC-1, A_{2B} adenosine receptors were shown to not only stimulate adenylate cyclase via coupling to Gs, but also stimulate PLC β via a GTP-binding protein of the Gq family resulting in accumulation of DAG and IP₃ (Feoktistov and Biaggioni, 1995; Linden et al., 1999; Feoktistov et al., 2002; Ryzhov et al., 2009). In the present study, we found that stimulation of adenylate cyclase by forskolin or activation of DAG-dependent pathways with PMA increased JunB protein levels and VEGF production. Further analysis employing inhibitors of PLC-linked pathways revealed their essential role in A_{2B} receptor-dependent regulation of both JunB and VEGF. Inhibition of PLC with U73122 reduced A_{2B} receptor-dependent JunB protein accumulation and VEGF secretion. The most prominent intracellular targets of DAG and the functionally analogous phorbol esters belong to the PKC family (Ron and Kazanietz, 1999). However, the broad-spectrum PKC inhibitor Gö6983 had no effect on the A_{2B} receptor-dependent increase in JunB protein levels and VEGF production. In addition to stimulation of PKC, PMA is known to activate CalDAG-GEF – Rap1 pathway eventually leading to activation of ERK (Stork and Dillon, 2005). In the current study, we demonstrated that this pathway is indeed activated by stimulation of A_{2B} receptors.

MOL #88567

Inhibition of NECA-induced Rap1 activation by the PLC inhibitor U73122 suggests that Rap1 and its activator CalDAG-GEF, which is known to respond to calcium and DAG (Kawasaki et al., 1998), are targets of A_{2B} receptor-activated PLC β . Although A_2 receptor-dependent stimulation of Rap1 has been previously reported in cells overexpressing A_2 receptors (Seidel et al., 1999; Schulte and Fredholm, 2003), this is the first evidence of PLC involvement in this process. Further downstream, inhibition of A_{2B} receptor-dependent stimulation of ERK with U0126 resulted in a partial inhibition of both JunB protein accumulation and VEGF production. Because complete inhibition of A_{2B} receptor-dependent upregulation of JunB and VEGF was not achieved even at U0126 concentrations that almost entirely blocked ERK activity, it is likely that additional pathways are involved in this mechanism. While stimulation of adenylate cyclase by forskolin also increased JunB protein levels and VEGF production, our data suggest involvement of PKA-independent pathways in this process because the PKA inhibitors with different mechanisms of action H-89 and Rp-cAMPS had no effect on the A_{2B} receptor-dependent increase in JunB protein levels and VEGF production. A_{2B} receptor-dependent stimulation of exchange proteins directly activated by cAMP, which are known to activate Rap1 (de Rooij et al., 1998), was recently demonstrated in endothelial cells (Fang and Olah, 2007). Whether this mechanism involved in A_{2B} receptor-dependent increase in JunB protein levels and VEGF production remains to be elucidated. Finally, the overexpression of dominant negative mutant of JunB or JunB knockdown with shRNA inhibited A_{2B} receptor-dependent increase in VEGF production, indicating an important role of JunB in this process. Thus, despite the apparent complexity and potential crosstalk between signaling pathways, our inhibitory analysis

MOL #88567

revealed a clear association and causal relationship between A_{2B} receptor-dependent regulation of JunB accumulation and VEGF secretion.

In conclusion, our study has demonstrated that A_{2B} adenosine receptor-dependent upregulation of JunB is a common feature shared by different cells known to be involved in angiogenesis. In addition to regulation of VEGF production examined in this study, JunB has been implicated in cell cycle regulation (Hess et al., 2004), endothelial cell morphogenesis (Licht et al., 2006), osteoblast differentiation (Kenner et al., 2004), myeloid cell differentiation (Passegue et al., 2001), mast cell degranulation, and cytokine release (Textor et al., 2007). Almost all of these events are reportedly regulated also by adenosine via A_{2B} receptors (Feoktistov and Biaggioni, 1997; Grant et al., 2001; Novitskiy et al., 2008; Ryzhov et al., 2011; Carroll et al., 2012; Feoktistov and Biaggioni, 1995; Auchampach et al., 1997). Therefore, it would be interesting to determine whether upregulation of JunB represents a common and important step in A_{2B} receptor-dependent regulation of these cell functions by extracellular adenosine.

MOL #88567

ACKNOWLEDGMENTS

We are grateful to Dr. N. Issaeva (Vanderbilt University, Nashville, TN) for help with immunofluorescence confocal microscopy and Dr. J. H. Butterfield (Mayo Clinic, Rochester, MN) for providing HMC-1 cell line. We also thank Dr. G.L. Semenza (Johns Hopkins Hospital, Baltimore, MD), Dr. P. A. D'Amore (Harvard University, Boston MA), Dr. M. Schorpp-Kistner (DKFZ - German Cancer Research Center, Heidelberg, Germany). and Dr. Mitsuyasu Kato (University of Tsukuba, Japan) for their generous gifts of human VEGF promoter-driven luciferase reporter, mouse VEGF promoter-driven luciferase reporter, mouse VEGF luciferase reporter with mutated AP-1 site, and dominant negative JunB mutant expression plasmids, respectively.

AUTHORSHIP CONTRIBUTIONS

Participated in research design: Ryzhov, Biktasova, Dikov, and Feoktistov

Conducted experiments: Ryzhov, Biktasova, Goldstein, Zhang

Performed data analysis: Ryzhov, Biktasova, and Feoktistov

Wrote or contributed to the writing of the manuscript: Ryzhov, Biktasova, Dikov, Biaggioni and Feoktistov

MOL #88567

REFERENCES

Adair TH (2005) Growth regulation of the vascular system: an emerging role for adenosine. *Am J Physiol* **289**:R283-R296.

Alchera E, Tacchini L, Imarisio C, Dal P C, De P C, Gammella E, Cairo G, Albano E and Carini R (2008) Adenosine-dependent activation of hypoxia-inducible factor-1 induces late preconditioning in liver cells. *Hepatology* **48**:230-239.

Auchampach JA, Jin X, Wan T C, Caughey G H and Linden J (1997) Canine mast cell adenosine receptors: Cloning and expression of the A₃ receptors and evidence that degranulation is mediated by the A_{2B} receptor. *Mol Pharmacol* **52**:846-860.

Bleasdale JE, Thakur N R, Gremban R S, Bundy G L, Fitzpatrick F A, Smith R J and Bunting S (1990) Selective inhibition of receptor-coupled phospholipase C-dependent processes in human platelets and polymorphonuclear neutrophils. *J Pharmacol Exp Ther* **255**:756-768.

Borrmann T, Hinz S, Bertarelli D C, Li W, Florin N C, Scheiff A B and Muller C E (2009) 1-alkyl-8-(piperazine-1-sulfonyl)phenylxanthines: development and characterization of adenosine A_{2B} receptor antagonists and a new radioligand with subnanomolar affinity and subtype specificity. *J Med Chem* **52**:3994-4006.

Carroll SH, Wigner N A, Kulkarni N, Johnston-Cox H, Gerstenfeld L C and Ravid K (2012) A_{2B} adenosine receptor promotes mesenchymal stem cell differentiation to osteoblasts and bone formation in vivo. *J Biol Chem* **287**:15718-15727.

MOL #88567

de Rooij J, Zwartkruis F J, Verheijen M H, Cool R H, Nijman S M, Wittinghofer A and Bos J L (1998) Epac is a Rap1 guanine-nucleotide-exchange factor directly activated by cyclic AMP. *Nature* **396**:474-477.

De Ponti C, Carini R, Alchera E, Nitti M P, Locati M, Albano E, Cairo G and Tacchini L (2007) Adenosine A_{2A} receptor-mediated, normoxic induction of HIF-1 through PKC and PI-3K-dependent pathways in macrophages. *J Leukoc Biol* **82**:392-402.

Dong W, Li Y, Gao M, Hu M, Li X, Mai S, Guo N, Yuan S and Song L (2012) IKK α contributes to UVB-induced VEGF expression by regulating AP-1 transactivation. *Nucleic Acids Res* **40**:2940-2955.

Fang Y and Olah M E (2007) Cyclic AMP-dependent, protein kinase A-independent activation of extracellular signal-regulated kinase 1/2 following adenosine receptor stimulation in human umbilical vein endothelial cells: role of exchange protein activated by cAMP 1 (Epac1). *J Pharmacol Exp Ther* **322**:1189-1200.

Feoktistov I and Biaggioni I (1995) Adenosine A_{2B} receptors evoke interleukin-8 secretion in human mast cells. An enprofylline-sensitive mechanism with implications for asthma. *J Clin Invest* **96**:1979-1986.

Feoktistov I and Biaggioni I (1997) Adenosine A_{2B} receptors. *Pharmacol Rev* **49**:381-402.

Feoktistov I, Biaggioni I and Cronstein B N (2009) Adenosine receptors in wound healing, fibrosis and angiogenesis. *Handb Exp Pharmacol* **193**:383-397.

MOL #88567

Feoktistov I, Goldstein A E, Ryzhov S, Zeng D, Belardinelli L, Voyno-Yasenetskaya T and Biaggioni I (2002) Differential expression of adenosine receptors in human endothelial cells: role of A_{2B} receptors in angiogenic factor regulation. *Circ Res* **90**:531-538.

Feoktistov I, Ryzhov S, Goldstein A E and Biaggioni I (2003) Mast cell-mediated stimulation of angiogenesis: cooperative interaction between A_{2B} and A₃ adenosine receptors. *Circ Res* **92**:485-492.

Forsythe JA, Jiang B H, Iyer N V, Agani F, Leung S W, Koos R D and Semenza G L (1996) Activation of vascular endothelial growth factor gene transcription by hypoxia-inducible factor 1. *Mol Cell Biol* **16**:4604-4613.

Fredholm BB, Ijzerman A P, Jacobson K A, Klotz K N and Linden J (2001) International Union of Pharmacology. XXV. Nomenclature and classification of adenosine receptors. *Pharmacol Rev* **53**:527-552.

Gessi S, Fogli E, Sacchetto V, Merighi S, Varani K, Preti D, Leung E, MacLennan S and Borea P A (2010) Adenosine modulates HIF-1 α , VEGF, IL-8, and foam cell formation in a human model of hypoxic foam cells. *Arterioscler Thromb Vasc Biol* **30**:90-97.

Grant MB, Davis M I, Caballero S, Feoktistov I, Biaggioni I and Belardinelli L (2001) Proliferation, migration, and ERK activation in human retinal endothelial cells through A_{2B} adenosine receptor stimulation. *Invest Ophthalmol Visual Sci* **42**:2068-2073.

Grant MB, Tarnuzzer R W, Caballero S, Ozeck M J, Davis M I, Spoerri P E, Feoktistov I, Biaggioni I, Shryock J C and Belardinelli L (1999) Adenosine receptor activation induces

MOL #88567

vascular endothelial growth factor in human retinal endothelial cells. *Circ Res* **85**:699-706.

Gschwendt M, Dieterich S, Rennecke J, Kittstein W, Mueller H J and Johannes F J (1996) Inhibition of protein kinase C μ by various inhibitors. Differentiation from protein kinase C isoenzymes. *FEBS Lett* **392**:77-80.

Hess J, Angel P and Schorpp-Kistner M (2004) AP-1 subunits: quarrel and harmony among siblings. *J Cell Sci* **117**:5965-5973.

Ikebe D, Wang B, Suzuki H and Kato M (2007) Suppression of keratinocyte stratification by a dominant negative JunB mutant without blocking cell proliferation. *Genes Cells* **12**:197-207.

Karin M, Liu Z and Zandi E (1997) AP-1 function and regulation. *Curr Opin Cell Biol* **9**:240-246.

Kawasaki H, Springett G M, Toki S, Canales J J, Harlan P, Blumenstiel J P, Chen E J, Bany I A, Mochizuki N, Ashbacher A, Matsuda M, Housman D E and Graybiel A M (1998) A Rap guanine nucleotide exchange factor enriched highly in the basal ganglia. *Proc Natl Acad Sci U S A* **95**:13278-13283.

Kenner L, Hoebertz A, Beil F T, Keon N, Karreth F, Eferl R, Scheuch H, Szremska A, Amling M, Schorpp-Kistner M, Angel P and Wagner E F (2004) Mice lacking JunB are osteopenic due to cell-autonomous osteoblast and osteoclast defects. *J Cell Biol* **164**:613-623.

MOL #88567

Lee CC, Chen S C, Tsai S C, Wang B W, Liu Y C, Lee H M and Shyu K G (2006) Hyperbaric oxygen induces VEGF expression through ERK, JNK and c-Jun/AP-1 activation in human umbilical vein endothelial cells. *J Biomed Sci* **13**:143-156.

Licht AH, Pein O T, Florin L, Hartenstein B, Reuter H, Arnold B, Lichter P, Angel P and Schorpp-Kistner M (2006) JunB is required for endothelial cell morphogenesis by regulating core-binding factor beta. *J Cell Biol* **175**:981-991.

Linden J, Thai T, Figler H, Jin X and Robeva A S (1999) Characterization of human A_{2B} adenosine receptors: radioligand binding, western blotting, and coupling to G_q in human embryonic kidney 293 cells and HMC-1 mast cells. *Mol Pharmacol* **56**:705-713.

Merighi S, Benini A, Mirandola P, Gessi S, Varani K, Leung E, Maclellan S, Baraldi P G and Borea P A (2005) A₃ adenosine receptors modulate hypoxia-inducible factor-1 α expression in human a375 melanoma cells. *Neoplasia (New York)* **7**:894-903.

Merighi S, Benini A, Mirandola P, Gessi S, Varani K, Leung E, Maclellan S and Borea P A (2006) Adenosine modulates vascular endothelial growth factor expression via hypoxia-inducible factor-1 in human glioblastoma cells. *Biochem Pharmacol* **72**:19-31.

Nesbitt SA and Horton M A (1992) A nonradioactive biochemical characterization of membrane proteins using enhanced chemiluminescence. *Anal Biochem* **206**:267-272.

Novitskiy SV, Ryzhov S, Zaynagetdinov R, Goldstein A E, Huang Y, Tikhomirov O Y, Blackburn M R, Biaggioni I, Carbone D P, Feoktistov I and Dikov M M (2008) Adenosine receptors in regulation of dendritic cell differentiation and function. *Blood* **112**:1822-1831.

MOL #88567

Pages G and Pouyssegur J (2005) Transcriptional regulation of the Vascular Endothelial Growth Factor gene--a concert of activating factors. *Cardiovasc Res* **65**:564-573.

Passegue E, Jochum W, Schorpp-Kistner M, Mohle-Steinlein U and Wagner E F (2001) Chronic myeloid leukemia with increased granulocyte progenitors in mice lacking junB expression in the myeloid lineage. *Cell* **104**:21-32.

Ramanathan M, Luo W, Csoka B, Hasko G, Lukashev D, Sitkovsky M V and Leibovich S J (2009) Differential regulation of HIF-1 α isoforms in murine macrophages by TLR4 and adenosine A_{2A} receptor agonists. *J Leukoc Biol* **86**:681-689.

Ramanathan M, Pinhal-Enfield G, Hao I and Leibovich S J (2007) Synergistic up-regulation of vascular endothelial growth factor (VEGF) expression in macrophages by adenosine A_{2A} receptor agonists and endotoxin involves transcriptional regulation via the hypoxia response element in the VEGF promoter. *Mol Biol Cell* **18**:14-23.

Ron D and Kazanietz M G (1999) New insights into the regulation of protein kinase C and novel phorbol ester receptors. *FASEB J* **13**:1658-1676.

Rothermel JD, Stec W J, Baraniak J, Jastorff B and Botelho L H (1983) Inhibition of glycogenolysis in isolated rat hepatocytes by the Rp diastereomer of adenosine cyclic 3',5'-phosphorothioate. *J Biol Chem* **258**:12125-12128.

Ryzhov S, Goldstein A E, Novitskiy S V, Blackburn M R, Biaggioni I and Feoktistov I (2012) Role of A_{2B} adenosine receptors in regulation of paracrine functions of stem cell antigen 1-positive cardiac stromal cells. *J Pharmacol Exp Ther* **341**:764-774.

MOL #88567

Ryzhov S, Novitskiy S V, Goldstein A E, Biktasova A, Blackburn M R, Biaggioni I, Dikov M M and Feoktistov I (2011) Adenosinergic regulation of the expansion and immunosuppressive activity of CD11b⁺Gr1⁺ cells. *J Immunol* **187**:6120-6129.

Ryzhov S, Novitskiy S V, Zaynagetdinov R, Goldstein A E, Carbone D P, Biaggioni I, Dikov M M and Feoktistov I (2008a) Host A_{2B} adenosine receptors promote carcinoma growth. *Neoplasia (New York)* **10**:987-995.

Ryzhov S, Zaynagetdinov R, Goldstein A E, Matafonov A, Biaggioni I and Feoktistov I (2009) Differential role of the carboxy-terminus of the A_{2B} adenosine receptor in stimulation of adenylate cyclase, phospholipase C β , and interleukin-8. *Purinergic Signal* **5**:289-298.

Ryzhov S, Zaynagetdinov R, Goldstein A E, Novitskiy S V, Dikov M M, Blackburn M R, Biaggioni I and Feoktistov I (2008b) Effect of A_{2B} adenosine receptor gene ablation on proinflammatory adenosine signaling in mast cells. *J Immunol* **180**:7212-7220.

Schmidt D, Textor B, Pein O T, Licht A H, Andrecht S, Sator-Schmitt M, Fusenig N E, Angel P and Schorpp-Kistner M (2007) Critical role for NF-kappaB-induced JunB in VEGF regulation and tumor angiogenesis. *EMBO J* **26**:710-719.

Schorpp-Kistner M, Wang Z Q, Angel P and Wagner E F (1999) JunB is essential for mammalian placentation. *EMBO J* **18**:934-948.

Schulte G and Fredholm B B (2003) The G_s-coupled adenosine A_{2B} receptor recruits divergent pathways to regulate ERK1/2 and p38. *Exp Cell Res* **290**:168-176.

MOL #88567

Seidel MG, Klinger M, Freissmuth M and Holler C (1999) Activation of mitogen-activated protein kinase by the A_{2A}-adenosine receptor via a rap1-dependent and via a p21^{ras}-dependent pathway. *J Biol Chem* **274**:25833-25841.

Shima DT, Kuroki M, Deutsch U, Ng Y S, Adamis A P and D'Amore P A (1996) The mouse gene for vascular endothelial growth factor. Genomic structure, definition of the transcriptional unit, and characterization of transcriptional and post-transcriptional regulatory sequences. *J Biol Chem* **271**:3877-3883.

Stork PJ and Dillon T J (2005) Multiple roles of Rap1 in hematopoietic cells: complementary versus antagonistic functions. *Blood* **106**:2952-2961.

Textor B, Licht A H, Tuckermann J P, Jessberger R, Razin E, Angel P, Schorpp-Kistner M and Hartenstein B (2007) JunB is required for IgE-mediated degranulation and cytokine release of mast cells. *J Immunol* **179**:6873-6880.

Textor B, Sator-Schmitt M, Richter K H, Angel P and Schorpp-Kistner M (2006) c-Jun and JunB are essential for hypoglycemia-mediated VEGF induction. *Ann N Y Acad Sci* **1091**:310-318.

Yin Y, Wang S, Sun Y, Matt Y, Colburn N H, Shu Y and Han X (2009) JNK/AP-1 pathway is involved in tumor necrosis factor-alpha induced expression of vascular endothelial growth factor in MCF7 cells. *Biomed Pharmacother* **63**:429-435.

Zeng D, Maa T, Wang U, Feoktistov I, Biaggioni I and Belardinelli L (2003) Expression and function of A_{2B} adenosine receptors in the U87MG tumor cells. *Drug Dev Res* **58**:405-411.

MOL #88567

FOOTNOTES:

This work was supported by National Institutes of Health National Heart, Lung and Blood Institute [grant R01HL095787] (to IF) and National Cancer Institute [grant R01CA138923] (to MMD and IF).

Reprint requests to: Sergey Ryzhov, MD, PhD, 360 PRB, Vanderbilt University, 2220
Pierce Ave, Nashville, TN 37232-6300. Phone: 615-936-1733, FAX: 615-936-1733,
email: sergey.v.ryzhov@vanderbilt.edu

MOL #88567

FIGURE LEGENDS

Figure 1. NECA-dependent upregulation of VEGF production is associated with an increase in VEGF transcription, AP-1 activity and JunB accumulation in various human and mouse cell types.

Human microvascular endothelial cells HMEC-1 (A, E, J, N), human mast cells HMC-1 (B, F, K, O), mouse cardiac Sca1⁺CD31⁻ stromal cells mCSC (C, G, L, P), and Lewis lung carcinoma cells LLC (D, H, M, Q) were either not transfected (A-D, N-Q), or transfected with plasmids encoding VEGF (E-H) or AP-1 (J-M) luciferase reporters and incubated in the absence (Basal) or presence of 10 μ M NECA for 6 (A-M) or 3 (N-Q) hours. VEGF release (A-D), VEGF (E-H) and AP-1 (J-M) reporter activities and JunB protein levels (N-Q) were analyzed as described in Methods. Values are presented as mean \pm SEM (n=3-10) in panels A-M. Asterisks indicate statistical difference (*p<0.05, **p<0.01, and ***p<0.001) compared to basal values by two-tailed unpaired *t* tests. Representative blots of 3-5 experiments are shown in panels N-Q.

Figure 2. Effects of NECA on the expression of members of the Jun family transcription factors in cells with adenosine-dependent regulation of VEGF.

Real-time RT-PCR analysis of mRNA encoding c-Jun, JunB and JunD in human microvascular endothelial cells (HMEC-1, panel A), human mast cells (HMC-1, panel B), mouse cardiac Sca1⁺CD31⁻ stromal cells (mCSC, panel C), and Lewis lung carcinoma cells (LLC, panel D) incubated in the absence (Basal) or presence of 10 μ M

MOL #88567

NECA for 60 minutes. Values are normalized to β -actin mRNA expression, and expressed as average of two determinations made in triplicate.

Figure 3. *A_{2B} adenosine receptors mediate an increase in JunB promoter-driven reporter activity and JunB protein accumulation in the nucleus.*

A, Real-time RT-PCR analysis of mRNA encoding adenosine receptor subtypes in human microvascular endothelial cells (HMEC-1), human mast cells (HMC-1), mouse cardiac Sca1⁺CD31⁻ stromal cells (mCSC), and Lewis lung carcinoma cells (LLC) was performed as described in Methods. Values are expressed as average of two determinations made in triplicate.

B, Pharmacological analysis of the role of A₂ adenosine receptor subtypes in regulation of JunB promoter-driven reporter activity in LLC cells. LLC cells were transiently transfected with JunB promoter-driven luciferase reporter and then incubated in the absence (Basal) or presence of the selective A_{2A} receptor agonist CGS 21680 (1 μ M), or the non-selective adenosine receptor agonist NECA (10 μ M) in the absence or presence of the selective A_{2B} receptor antagonist PSB603 (100 nM) for 3 hours. Values are presented as mean \pm SEM (n=3). Asterisk indicates statistical difference (*p<0.05) compared to basal levels.

C, Effect of increasing concentrations of the selective A_{2B} receptor antagonist PSB603 on JunB protein levels in LLC cells stimulated with 10 μ M NECA for 3 hours. A representative blot of 3 experiments is shown.

D, Pharmacological analysis of the role of A_{2B} adenosine receptors in regulation of JunB protein accumulation in LLC nuclei. LLC cells were incubated in the absence (Basal) or

MOL #88567

presence of the non-selective adenosine receptor agonist NECA (10 μ M) in the absence or presence of the selective A_{2B} receptor antagonist PSB603 (100 nM) for 3 hours. Representative micrographs of anti-JunB-stained LLC cells (green) and nuclei stained with DAPI (blue) from 3 experiments are shown.

E, Quantification of immunofluorescence data shown in panel D. Fluorescence intensity was measured in seven randomly chosen cells per slide using ImageJ and the corrected total cell fluorescence (CTCF) values are presented as mean \pm SEM. Asterisks indicate statistical difference (***) p <0.001) compared to basal levels.

Figure 4. Stimulation of A_{2B} receptor-linked signaling pathways increases VEGF secretion and JunB protein levels.

A, VEGF release from HMEC-1 cells incubated in the absence (Basal) or presence of 10 μ M NECA, 1 μ M CGS 21680, 1 μ M forskolin, or 10 nM PMA for 6 hours. Values are expressed as mean \pm SEM (n=6). Asterisks indicate significant difference (** p <0.01, one-way ANOVA with Dunnett's post-test) and ns indicates non-significant difference compared to basal levels.

B, Western blot analysis of JunB protein levels in HMEC-1 cells incubated in the absence (Basal) or presence 10 μ M NECA, 1 μ M CGS 21680, 1 μ M forskolin, or 10 nM PMA for 3 hours. Arrows indicate positions of JunB and β -actin, the latter used as a loading control. A representative blot of 3 experiments is shown.

C, Graphic representation of data shown in panel B quantified by densitometry and expressed as relative density of JunB bands normalized to corresponding β -actin bands.

MOL #88567

Figure 5. Effects of inhibitors of protein kinases A and C on A_{2B} receptor-dependent increase in VEGF secretion and JunB protein levels.

A, VEGF secretion from HMEC-1 cells incubated in the absence (Basal) or presence of 10 μ M NECA, or in the presence of NECA and 1 μ M H-89, 100 μ M Rp-cAMPS, or 1 μ M Gö6983 for 6 hours. Values are presented as mean \pm SEM (n=3).

B, Western blot analysis of JunB protein levels in HMEC-1 cells incubated in the absence (Basal) or presence of 10 μ M NECA, or in the presence of NECA and 1 μ M H-89, 100 μ M Rp-cAMPS, or 1 μ M Gö6983 for 3 hours. Arrows indicate positions of JunB and β -actin, the latter used as a loading control. A representative blot of 3 experiments is shown.

C, Graphic representation of data shown in panel B quantified by densitometry and expressed as relative density of JunB bands normalized to corresponding β -actin bands.

Figure 6. Effects of PLC and MEK inhibition on VEGF secretion and JunB levels in HMEC-1 cells.

A, Effects of the PLC inhibitor U73122 (closed circles) and its inactive control analog U73343 (open circles) on VEGF secretion from cells stimulated with 10 μ M NECA. In the absence of inhibitors, 10 μ M NECA increased concentrations of VEGF in the medium from 47 \pm 1 to 138 \pm 1 pg/10⁶ cells. Values are presented as mean \pm SEM (n=6).

B, Effects of increasing concentrations of the MEK inhibitor UO126 (closed circles) and its inactive control analog UO124 (open circles) on VEGF secretion from cells stimulated with 10 μ M NECA. Values are presented as mean \pm SEM (n=3).

MOL #88567

C, Western blot analysis of JunB protein levels in HMEC-1 cells incubated in the absence (Basal) or presence of 10 μ M NECA, or in the presence of NECA and 10 μ M U73122, 10 μ M U73343, 1 μ M UO126 or 1 μ M UO124 for 3 hours. Arrows indicate positions of JunB and β -actin, the latter used as a loading control. A representative blot of 3 experiments is shown.

D, Graphic representation of data shown in panel C quantified by densitometry and expressed as relative density of JunB bands normalized to corresponding β -actin bands.

Figure 7. Effect of PLC inhibition on adenosine-dependent Rap1 activation.

A. Western blot analysis of active GTP-bound form of Rap1 obtained by GST-Ral-GDS pulldown before and 5, 10, and 15 minutes after stimulation of HMEC-1 cells with 10 μ M NECA in the absence (Control) and presence of 10 μ M U73122. Total Rap1 protein levels in corresponding cell lysate aliquots are shown in bottom panels. Representative blots of 3 experiments are shown.

B. Graphic representation of data shown in panel A quantified by densitometry and expressed as a percentage of corresponding levels in resting cells normalized to total Rap-1 protein levels used as internal control.

Figure 8. Role of JunB in A_{2B} receptor -dependent VEGF production.

A. Effect of NECA on JunB binding to the VEGF promoter. ChIP analysis was performed using an antibody specific for JunB (IP: JunB) and IgG as a non-specific control (IP: ns). Specific primer sets were used for the promoter region harboring the AP-

MOL #88567

1 site (-1140 to -733). JunB binding to the VEGF promoter region between -1140 and -733 was detected and was enhanced in LLC cells treated with 10 μ M NECA for 3 h.

B. Effects of AP-1 site mutation and dominant negative JunB on VEGF reporter activity.

The role of JunB in A_{2B} receptor-dependent regulation of the VEGF gene promoter was studied in LLC cells transiently cotransfected with VEGF luciferase reporter together with plasmid encoding dominant negative JunB (indicated on graph as DNJunB) or with an empty vector (mock). A set of LLC cells was also transfected with VEGF luciferase reporter containing the mutated AP-1 site at -1093 (indicated on graph as mutAP-1). Twenty-four hours after transfections, cells were incubated in the absence (Basal) or presence of 10 μ M NECA for an additional 6 hours. Values are presented as mean \pm SEM (n=3). Asterisks indicate statistical difference (**p<0.01) compared to basal levels, dagger indicates statistical difference (\dagger p<0.05) compared to mock controls by one-way ANOVA with Bonferroni post-test.

C. Expression of JunB and DNJunB in LLC cells stably transfected with plasmid encoding DNJunB or with an empty vector (mock). Western blot analysis was performed using antibodies against a common epitope in the sequences of JunB and DNJunB. Arrows indicate positions of JunB and DNJunB. Immunostaining of β -tubulin was used as a loading control.

D. Effect of the expression of dominant negative JunB on VEGF secretion. The role of JunB in A_{2B} receptor-dependent regulation of VEGF secretion was studied in LLC cells stably transfected with plasmid encoding DNJunB or with an empty vector (mock) by measuring VEGF release from cells incubated in the absence (Basal) or presence of 10 μ M NECA for 6 hours. Values are presented as mean \pm SEM (n=3). Asterisks indicate

MOL #88567

statistical difference (* $p < 0.05$, and *** $p < 0.001$) compared to basal levels, daggers indicate statistical difference ($^{\dagger\dagger}p < 0.01$) compared to mock controls by one-way ANOVA with Bonferroni post-test.

E. Efficacy of JunB silencing after stable lentiviral transfection of LLC cells with different shRNA constructs (shRNA1-5) compared to shRNA non-targeting (NT) and empty vector (EV) controls. Upper panels show representative Western blots of basal levels of targeted JunB protein and β -tubulin loading controls. Lower panel is a graphic representation of data expressed as relative density of JunB bands normalized to corresponding β -tubulin bands and NT control.

F. Real-time RT-PCR analysis of JunB mRNA levels in LLC cells stably transfected with lentiviral vectors encoding shRNA5 or non-targeting shRNA (NT control). Cells were incubated in the absence (Basal) or presence of 10 μ M NECA for 60 minutes. Values are normalized to β -actin mRNA expression and expressed as average of two determinations made in triplicate.

G. Effect of JunB knockdown on VEGF secretion. The role of JunB in A_{2B} receptor-dependent regulation of the VEGF secretion was studied in LLC cells stably expressing JunB silencing shRNA5 or non-targeting shRNA (NT control) incubated in the absence (Basal) or presence of 10 μ M NECA for 6 hours. Values are presented as mean \pm SEM ($n=3$). Asterisks indicate statistical difference (* $p < 0.05$, and *** $p < 0.001$) compared to basal levels, daggers indicate statistical difference ($^{\dagger\dagger}p < 0.001$) compared to NT controls by one-way ANOVA with Bonferroni post-test.

MOL #88567

Figure 9. Schematic representation of A_{2B} receptor-stimulated intracellular pathways involved in regulation of VEGF.

A_{2B} adenosine receptors ($A_{2B}AR$) are coupled to adenylylate cyclase (AC) via Gs-proteins. Activation of this pathway results in accumulation of cAMP and stimulation of protein kinase A (PKA). $A_{2B}AR$ are coupled also to phospholipase C β (PLC) via a GTP-binding protein of the Gq family. Activation of this pathway results in accumulation of diacylglycerol (DAG) and inositol trisphosphate (IP $_3$) and the latter triggers mobilization of calcium from intracellular stores (Feoktistov and Biaggioni, 1995).

In this study, we present evidence that $A_{2B}AR$ increase JunB protein levels and VEGF production via stimulation of PLC and ERK which are possibly linked by the calcium diacylglycerol guanine nucleotide exchange factor (CalDAG-GEF) – Ras-proximate-1 (Rap1) pathway. Phorbol 12-myristate 13-acetate (PMA), an activator of protein kinases C (PKC) and CalDAG-GEF, also increased JunB protein levels and VEGF production. However, the broad spectrum PKC inhibitor Gö6983 had no effect on the $A_{2B}AR$ -dependent increase in JunB protein levels and VEGF production. In contrast, the PLC inhibitor U73122 inhibited the $A_{2B}AR$ -dependent Rap1 activation, increase in JunB protein levels, and VEGF production. The mitogen-activated protein kinase kinase (MEK) inhibitor U0126 blocked the $A_{2B}AR$ -dependent stimulation of extracellular-signal-regulated kinase (ERK) and inhibited an increase in JunB protein levels and VEGF production. Stimulation of AC by forskolin also increases JunB protein levels and VEGF production. Broken arrows in the diagram signify potential effects of cAMP. These effects are PKA-independent because the PKA inhibitors with different mechanisms of action H-89 and Rp-cAMPS had no effect on the $A_{2B}AR$ -dependent increase in JunB

MOL #88567

protein levels and VEGF production. Finally, the overexpression of a dominant negative mutant of JunB (DNJunB) inhibited A_{2B}AR-dependent increase in VEGF transcription and secretion indicating an important role of JunB in this process.

MOL #88567

Table. Primers for RT-PCR used in this study.

Target	Forward primer (5'-3')	Reverse primer (5'-3')
<i>Mouse</i>		
JunB	TAAAGAGGAACCGCAGACCGTA	AGTGTCTTCACCTTGTCCTCCA
JunD	AGTTGGACTCCACACATCCCAT	TGTCAGTTTCACAGGGTGGAGT
c-Jun	GGTGGCACAGCTTAAGCAGAAA	TCTCTGTCGCAACCAGTCAAGT
β -actin	AGTGTGACGTTGACATCCGTA	GCCAGAGCAGTAATCTCCTTCT
<i>Human</i>		
JunB	TGGAACAGCCCTTCTACCAC	GGTTTCAGGAGTTTGTAGTC
JunD	GCCTCATCATCCAGTCCAAC	CCACCTTGGGGTAGAGGAAC
c-Jun	TGACTGCAAAGATGGAAACG	CAGGGTCATGCTCTGTTTCA
β -actin	CGCCCCAGGCACCAGGGC	GGCTGGGGTGTTGAAGGT

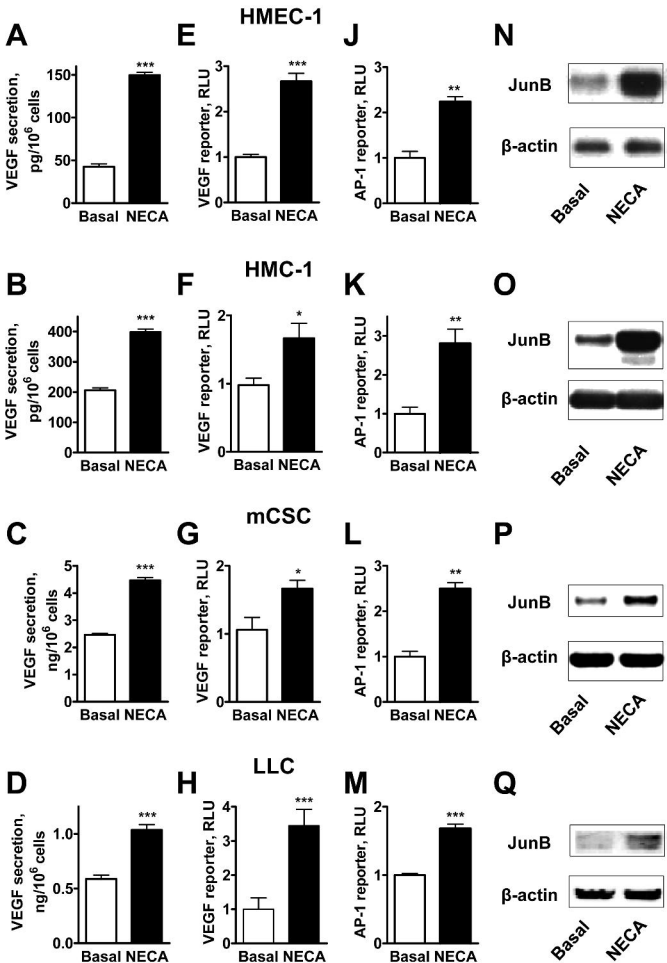


Figure 1

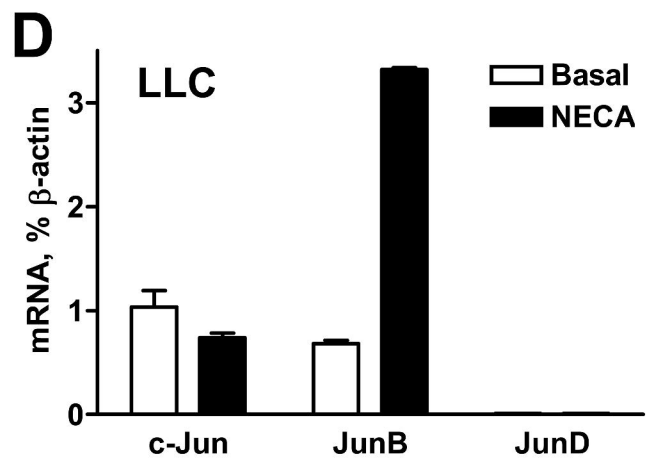
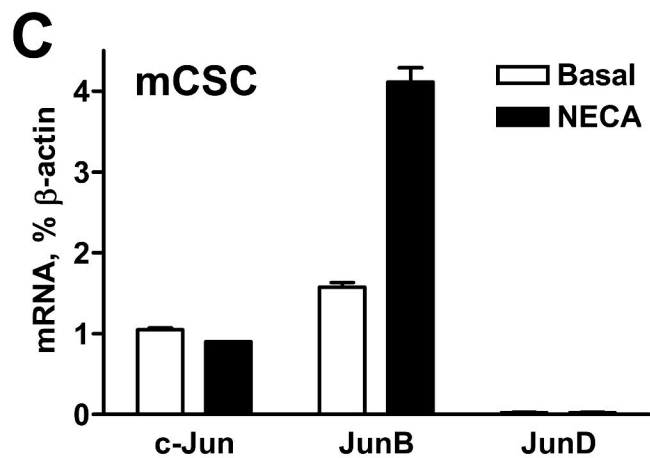
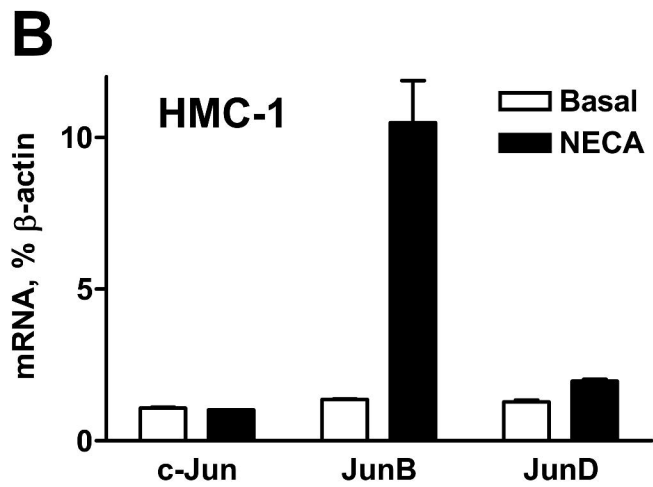
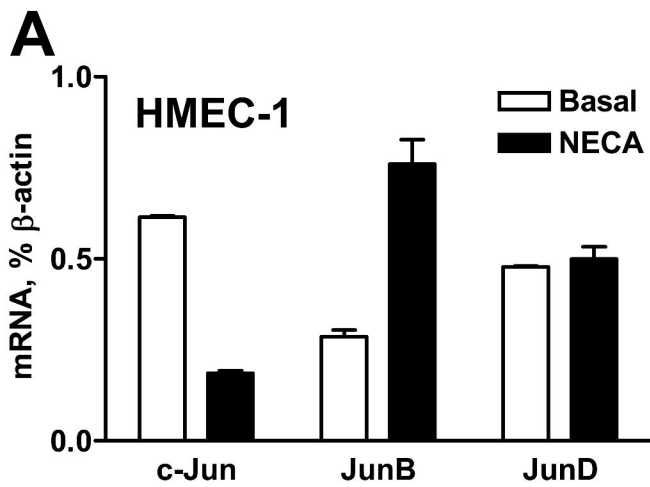


Figure 2

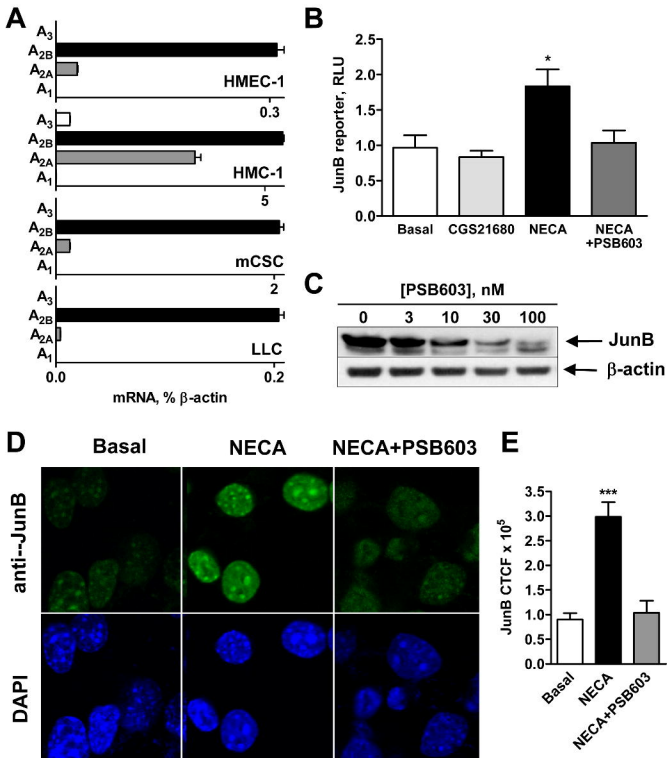


Figure 3

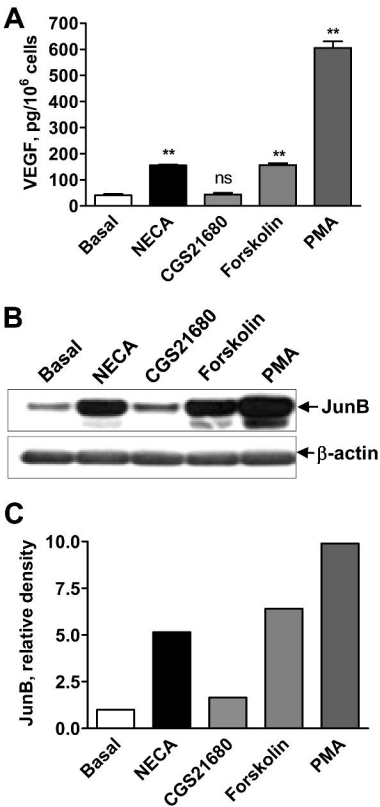


Figure 4

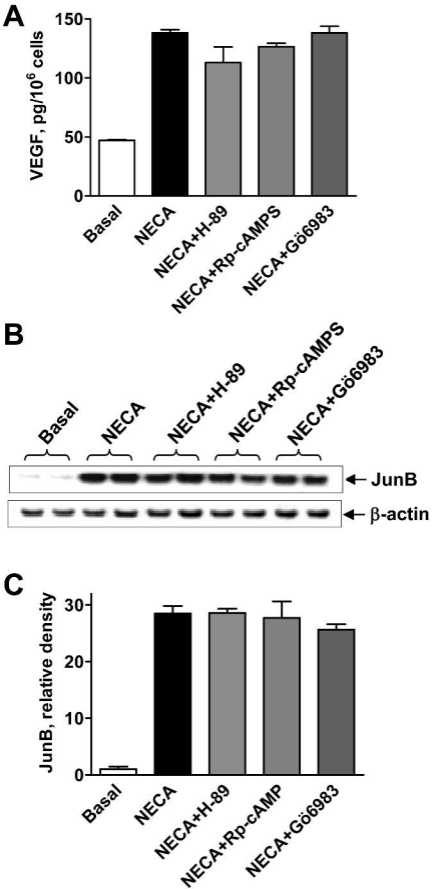


Figure 5

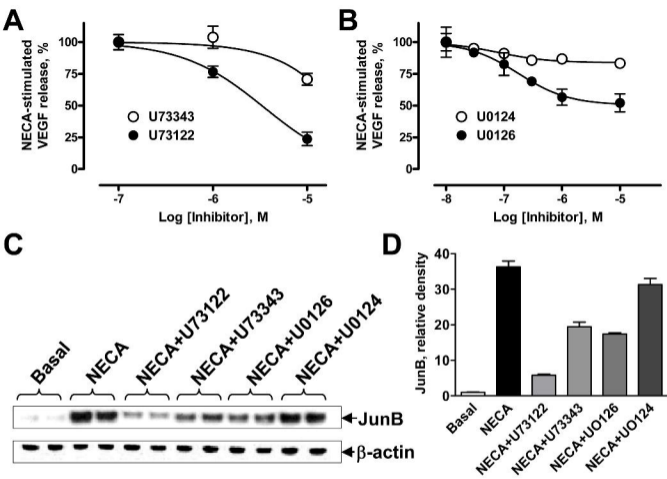


Figure 6

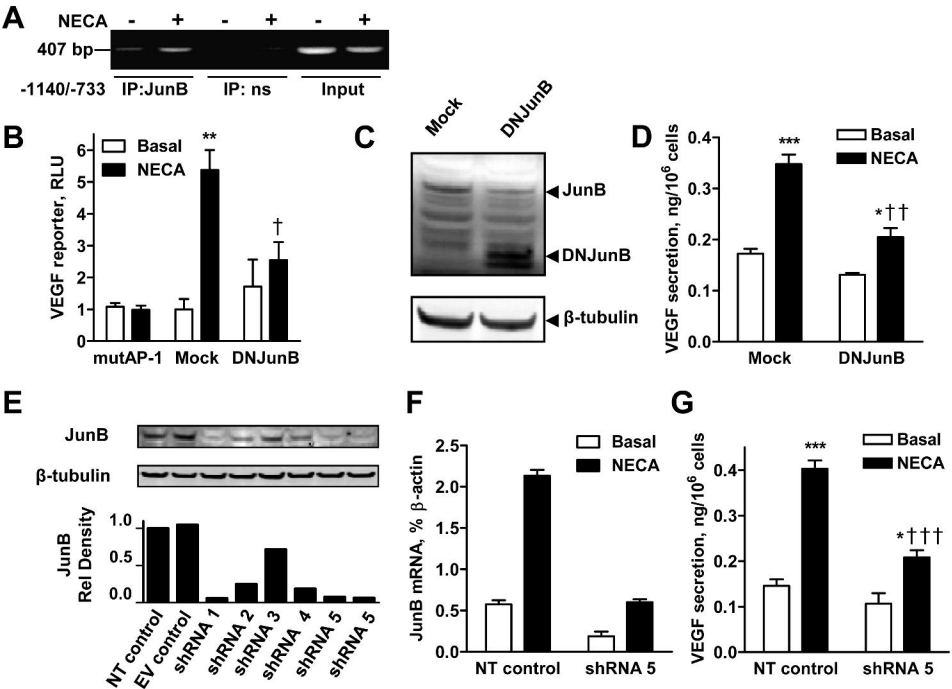


Figure 8

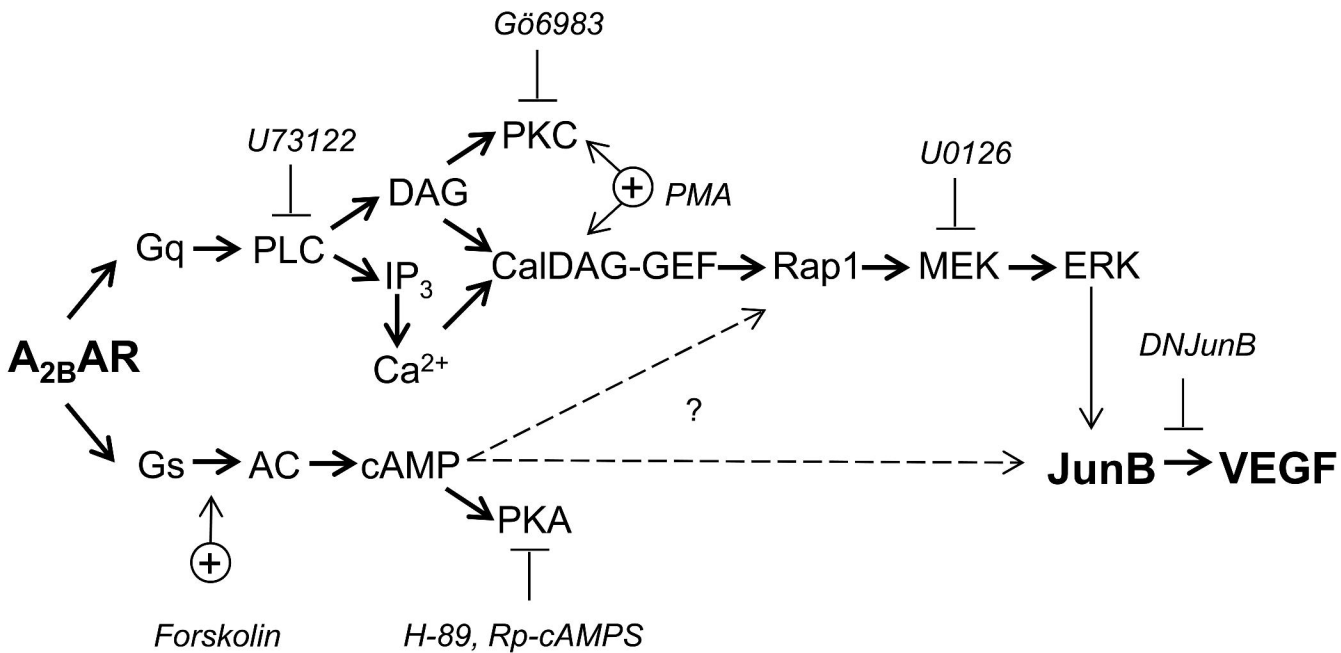


Figure 9

Molecular Pharmacology
Supplemental figures

Role of JunB in Adenosine A_{2B} Receptor-mediated VEGF Production

Sergey Ryzhov, Asel Biktasova, Anna E. Goldstein, Qinkun Zhang, Italo Biaggioni, Mikhail M.

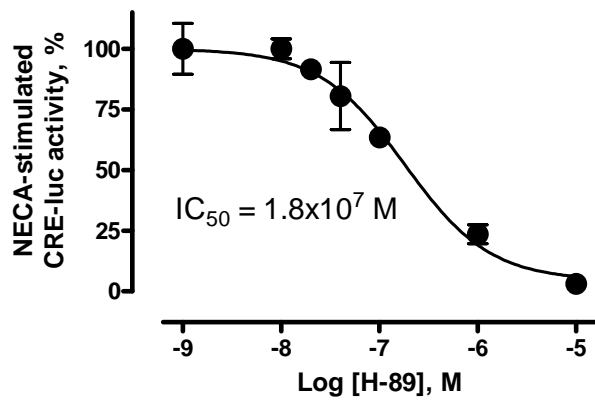
Dikov, Igor Feoktistov

Divisions of Cardiovascular Medicine (QZ, IF, SR) and Clinical Pharmacology (AEG, IB),

Departments of Cancer Biology (AB, MMD), Medicine (AEG, QZ, IB, IF, SR) and

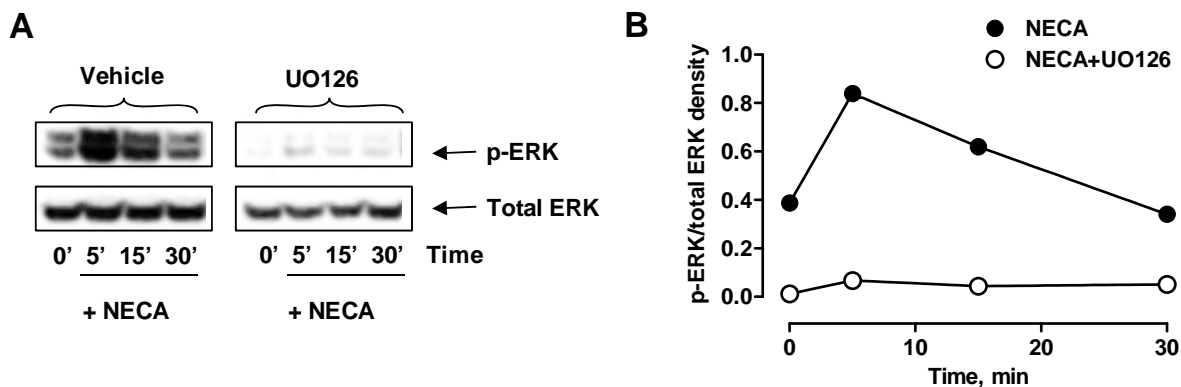
Pharmacology (IB, IF)

Vanderbilt University, Nashville, TN 37232.



Supplemental Figure 1. *Effect of the protein kinase A inhibitor H-89 on NECA-induced cAMP response element (CRE)-driven luciferase reporter activity in HMEC-1 cells.*

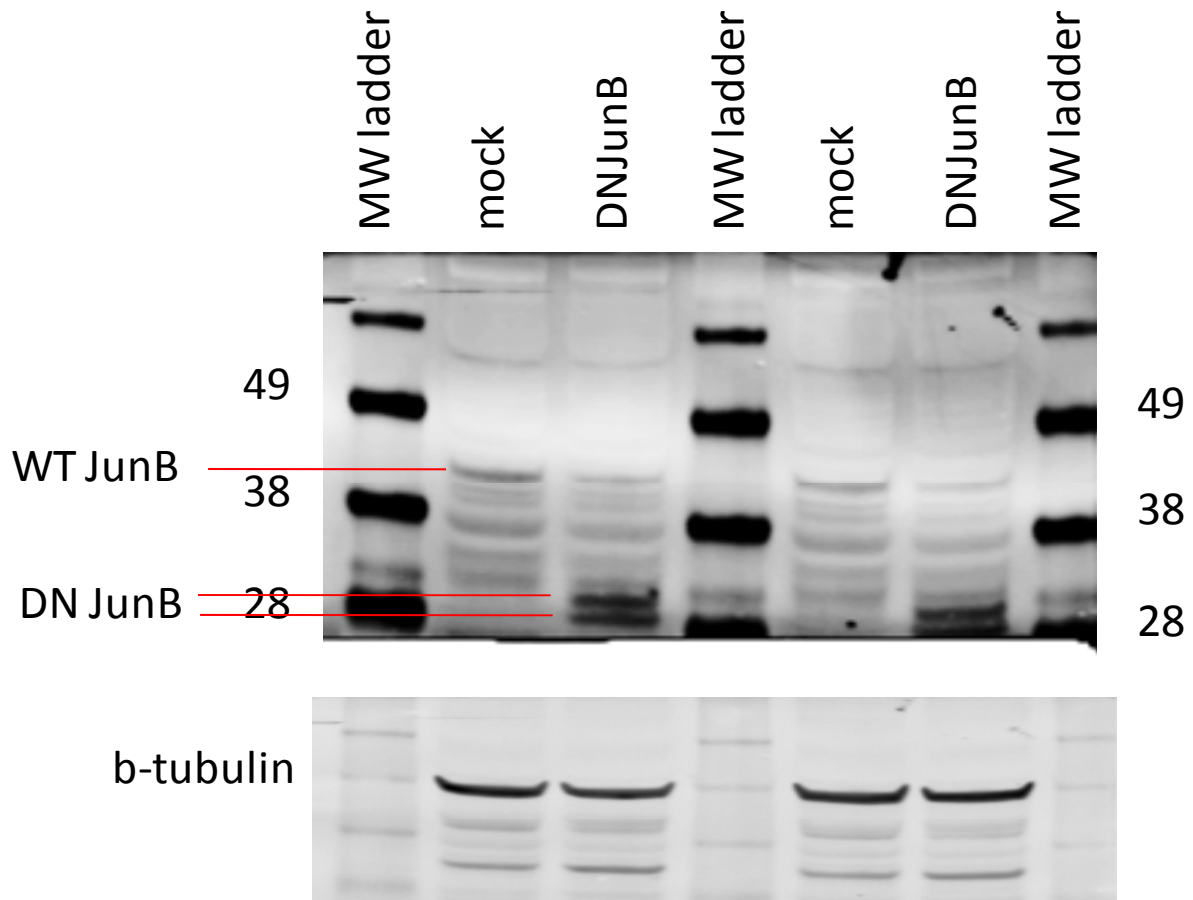
HMEC-1 cells transfected with a CRE reporter were incubated in the absence or presence of 10 μ M NECA in the absence or presence of increasing concentrations of H-89 for 6 hours. H-89 was added to cells 30 min before addition of NECA. Potency of H-89 on cAMP/PKA signaling transduction in HMEC-1 cells was determined as IC₅₀ from concentration-response curve of H-89 effects on NECA-stimulated CRE luciferase reporter activity. Values are presented as mean \pm SEM (n=3).



Supplemental Figure 2. Effect of the MEK inhibitor UO126 on NECA-induced ERK activation in HMEC-1 cells.

A, Time course of ERK activation by NECA in HMEC-1 cells in the absence (Vehicle) or presence of 1 μ M UO126. Cells were stimulated with 10 μ M NECA for indicated periods of time. ERK activation was determined by immunoblotting with antibody specific for phosphorylated ERK. Total ERK was used as a loading control. A representative blot of 3 experiments is shown.

B, Levels of phosphorylated ERK quantified from Western blot data by densitometry and expressed as percentage of corresponding levels in resting cells in the absence of UO126 normalized to total ERK levels.



Supplemental Figure 3. Expression of JunB and DNJunB in LLC cells stably transfected with plasmid encoding DNJunB or with an empty vector (mock).

Western blot analysis was performed using antibodies against a common epitope in the sequences of JunB and DNJunB. Molecular weight range is shown on both sides of gel. Red lines indicate positions of JunB and DNJunB. Immunostaining of β -tubulin was used as a loading control.